

# Controlled Covalent Self-Assembly of a Homopolymer for Multiscale Materials Engineering

Xiangyang Bai, Qingxue Sun, Hao Cui, Luis P. B. Guerzoni, Stefan Wuttke, Fabian Kiessling, Laura De Laporte, Twan Lammers, and Yang Shi\*

Polymer self-assembly is a crucial process in materials engineering. Currently, almost all polymer self-assembly is limited to non-covalent bonding methods, even though these methods have drawbacks as they require complicated synthesis techniques and produce relatively unstable structures. Here, a novel mechanism of covalent polymer self-assembly is discovered and employed to address drawbacks of non-covalent polymer self-assembly. A simple ketone homopolymer is found to self-assemble into nano- to macroscale hydrogels during covalent crosslinking. In contrast to non-covalent self-assembly, the covalent self-assembly is independent of and unaffected by solvent conditions (e.g., polarity and ionic strength) and does not require additional agents, e.g., organic solvents and surfactants. The covalent polymer self-assembly is subjected to a new mechanism of control by tuning the covalent crosslinking rate. This leads to nanogels with an unprecedented and tightly controlled range of dimensions from less than 10 nm to above 100 nm. Moreover, the crosslinking rate also regulates the assembly behavior of microgels fabricated by microfluidics. The microgels self-assemble into granular fibers, which is 3D printed into stable porous scaffolds. The novel covalent polymer assembly method has enormous potential to revolutionize multiscale materials fabrication for applications in drug delivery, tissue engineering, and many other fields.

#### 1. Introduction

Self-assembly plays a crucial role in nature and materials science.[1] In nature, biomolecules self-assemble into organelles which further organize into cells and multicellular living organisms. Similarly, selfassembly is used in materials synthesis to organize small, independent units into increasingly complex structures and materials.[2-4] One particularly popular molecular unit is polymers which have been used to make structures such as nanoparticles, fibers, and hydrogels.[5-9] These materials, even though they are crucial in many fields (particularly in biomedical applications), have fundamental limitations: current methods only report polymer self-assembly by weak non-covalent interactions, like hydrophobic, electrostatic, or  $\pi$ – $\pi$  stacking interactions and hydrogen bonding,[1] which are all dangerously sensitive to environmental conditions such as solvent polarity, temperature, ionic strength, pH, and co-solutes. Furthermore,

X. Bai, Q. Sun, H. Cui, F. Kiessling, T. Lammers, Y. Shi Uniklinik RWTH Aachen and Helmholtz Institute for Biomedical Engineering RWTH Aachen University 52074 Aachen, Germany E-mail: yshi@ukaachen.de

L. P. B. Guerzoni, L. De Laporte DWI-Leibniz Institute for Interactive Materials 52074 Aachen, Germany

S. Wuttke
BCMaterials
Basque Center for Materials

UPV/EHU Science Park Leioa 48940, Spain

The ORCID identification number(s) for the author(s) of this article can be found under https://doi.org/10.1002/adma.202109701.

© 2022 The Authors. Advanced Materials published by Wiley-VCH GmbH. This is an open access article under the terms of the Creative Commons Attribution-NonCommercial-NoDerivs License, which permits use and distribution in any medium, provided the original work is properly cited, the use is non-commercial and no modifications or adaptations are made.

S. Wuttke Ikerbasque Basque Foundation for Science Bilbao 48013, Spain

L. De Laporte Institute of Applied Medical Engineering Department of Advanced Materials for Biomedicine RWTH Aachen University 52074 Aachen, Germany

L. De Laporte
Institute for Technical and Macromolecular Chemistry
RWTH Aachen University
52074 Aachen, Germany
T. Lammers
Department of Pharmaceutics
Utrecht University

Utrecht 3584 CG, The Netherlands T. Lammers Department of Targeted Therapeutics University of Twente Enschede 7500 AE, The Netherlands

DOI: 10.1002/adma.202109701

and-conditions) on Wiley Online Library for rules of use; OA articles are governed by the applicable Creative Commons

www.advancedsciencenews.com

www.advmat.de



Scheme 1. Illustration of the covalent crosslinking-driven self-assembly (COSA) of a homopolymer. A) Controlled covalent assembly of the homopolymer (blue) with a chemical crosslinker (orange) to organize into nano- to macroscale hydrogels. B,C) The COSA is featured by its tight control via tuning the crosslinking rate: B) it leads to nanogels with an unprecedented range of size modulation from below 10 nm to above 100 nm and C) it enables self-assembly of microscale gels into granular fibers for direct 3D printing of porous scaffolds.

even if these conditions are carefully optimized to stabilize the polymer assembly, controlling the architecture of the resulting complex is exceedingly difficult, further complicating the synthesis or even making it impossible to produce the target structure without destroying the polymer constituents. Noncovalent polymer crosslinking is self-limiting—a different method is highly desired. A logical solution is the development of polymer self-assembly triggered and controlled by covalent crosslinking. Covalent self-assembly is an important concept in materials engineering which has been previously explored with small molecules<sup>[10]</sup> and peptides.<sup>[11,12]</sup>

We here report a covalent polymer self-assembly as a novel strategy to synthesize multiscale hierarchical gel networks (Scheme 1). The new approach, coined as covalent crosslinking-driven self-assembly (COSA), is exemplified by a unique ketone homopolymer which shows a previously unknown self-assembly behavior during crosslinking with dihydrazide crosslinkers. The COSA has been shown to address the drawbacks of non-covalent polymer self-assembly and effectively produces nano- to macroscale hydrogels with simple protocols and tight control of physico-chemical properties. The COSA is flexibly modulated by a new controlling strategy, enabling the fabrication of materials which are challenging to produce with previously existing methods. Our findings represent a new strategy to induce and control polymer self-assembly, and we believe it will truly transform the synthesis of hydrogel materials for various biomedical applications.

## 2. Results and Discussion

#### 2.1. Ketone Homopolymer Synthesis and Crosslinking

As the first step, we establish aqueous reversible addition-fragmentation chain transfer (RAFT) polymerization [13] for the simplest ketone-bearing methacrylamide monomer, N-(2-oxopropyl)methacrylamide (OPMA). The monomer conversion reaches 98% at 24 h, and pOPMA with an  $M_n$  of 8.5 kDa and  $\mathcal D$  of 1.1 is obtained (Figure 1A and Figures S1 and S2, Supporting Information). The product is highly soluble in water and organic solvents (Figure 1B). It is interesting to note that when OPMA is polymerized by free radical polymerization, undesired gelation of the polymerization is induced at different monomer concentrations and monomer/initiator ratios. The gelled solid products cannot be dissolved in commonly used aqueous and organic solvents (Figure 1A,B and Figure S3, Supporting Information).

It is commonly observed that crosslinking of homopolymers leads to random aggregation and macroscale gelation. However, pOPMA undergoes highly controlled self-assembly to form hydrogels at nano- to macroscale. pOPMA nanogels are directly synthesized via crosslinking of the polymer with adipic acid dihydrazide (ADH, Figure 1C). During hydrazone bond formation between pOPMA and ADH, a fraction of crosslinking occurs intermolecularly, which leads to self-assembly of polymer chains (Figure 1D). Our work shows that at low degrees of crosslinking (DC), the self-assembly is completed at the nanoscale and

conditions) on Wiley Online Library for rules of use; OA articles are governed by the applicable Creative Commons



www.advmat.de

A B H<sub>2</sub>O HCI NaOH MeOH ACN DMSO DMF DMAc DCM ACPA, CTCA RAFT polymerization HN HN **ACPA** Free radical polymerization **OPMA** pOPMA C COSA Low crosslinking HN + 2 H<sub>2</sub>O H+ or aniline COSA High crosslinking

Figure 1. Polymerization of OPMA and covalent crosslinking-driven self-assembly (COSA) of pOPMA. A) Synthesis schemes of pOPMA via RAFT and free radial polymerization. ACPA: 4,4'-azobis(4-cyanopentanoic acid), free-radical initiator. CTCA: 4-((((2-carboxyethyl)thio)carbonothioyl)-thio)-4-cyanopentanoic acid, RAFT chain transfer agent. B) Solubilization of products from RAFT (upper) and free-radical (bottom) polymerization of OPMA in aqueous and organic solvents. C) Reaction scheme of covalent crosslinking of pOPMA (in blue) with adipic acid dihydrazide (ADH, in orange), which is catalyzed by H+ or aniline. D) Schematic depiction of covalent self-assembly of pOPMA forming nanogels at low degrees of crosslinking (above), and at high degrees of crosslinking (below), the nanogels further self-assemble into macroscale hydrogels.

well-defined nanogels are yielded. At higher degrees of crosslinking, the nanogels undergo interparticle crosslinking to form micro- and macroscale hydrogels (Figure 1D).

### 2.2. COSA Leads to Nano- to Macroscale Hydrogels

We first demonstrate the nanogel formation via the COSA of pOPMA. The polymer at 15 mgmL<sup>-1</sup> is crosslinked with ADH in water at pH 5.0. The DC is 20%, i.e., the feed molar ratio between hydrazide and ketone is 1/5. The crosslinking results in an opalescent dispersion (Figure 2a). The sample is characterized by cryo field-emission scanning electron microscopy (CryoSEM) and dynamic light scattering (DLS). Both techniques support well-defined nanogel formation (Figure 2b,c). As shown by CryoSEM (Figure 2b), nanogels of a spherical morphology were obtained via COSA of pOPMA. Spherical nanoparticles of small molecules have also been fabricated via covalent self-assembly.<sup>[10,14]</sup> In our approach, the polymer chains undergo intermolecular crosslinking during hydrazone formation and this leads to spherical nanogel formation. The reaction is highly efficient and after the nanogelation residual free ADH and pOPMA are not detected (Figure S4, Supporting Information). The COSA of pOPMA occurs in solvents with different polarities (water, dimethyl sulfoxide (DMSO), and water/DMSO co-solvents, Figure S5, Supporting Information) and at different temperatures (Figure S6, Supporting Information), as well as at different polymer concentrations (Figure S7, Supporting Information), degrees of crosslinking (Figure S8, Supporting Information), and with pOPMA of different molecular weights (Figure S9, Supporting Information).

pOPMA nanogels are stable after different treatments, i.e., with an organic solvent (DMSO), surfactant (sodium dodecyl sulfate, SDS), salts (NaCl, KCl, Na2HPO4, and KH2PO4), hydrogen bond interrupter (urea), heating, and ultrasound (Figure S10, Supporting Information). These findings indicate that the nanogels are not based on weak non-covalent interactions but covalent bonds. Furthermore, adding SDS, salts, and urea during the COSA of pOPMA does not affect the size of the nanogels, showing that the self-assembly process of pOPMA is independent of the common non-covalent interactions (i.e., hydrophobic, charge and hydrogen bonding, Figure 2d,e). Also, removal of the chain transfer agent end group on pOPMA did not affect the size of formed nanoparticles (Figure S11, Supporting Information). pOPMA nanogels show high colloidal stability for more than a month at 4 °C and room temperature (Figure S12, Supporting Information). To assess whether multiple pOPMA chains assemble during COSA and the efficiency of self-assembly, we monitor the self-assembly process of pOPMA by Förster resonance energy transfer (FRET, Figure 2f) with Alexa-555- and Alexa-647-labeled pOPMA (Figure S13, Supporting Information). The FRET effect between the two fluorophores gradually increases during COSA, illustrating that multiple polymer chains assemble together (Figure 2g) and this process plateaus at 10 h of reaction (Figure S14, Supporting Information).

and-conditions) on Wiley Online Library for rules of use; OA articles are governed by the applicable Creative Commons License

www.advancedsciencenews.com

www.advmat.de

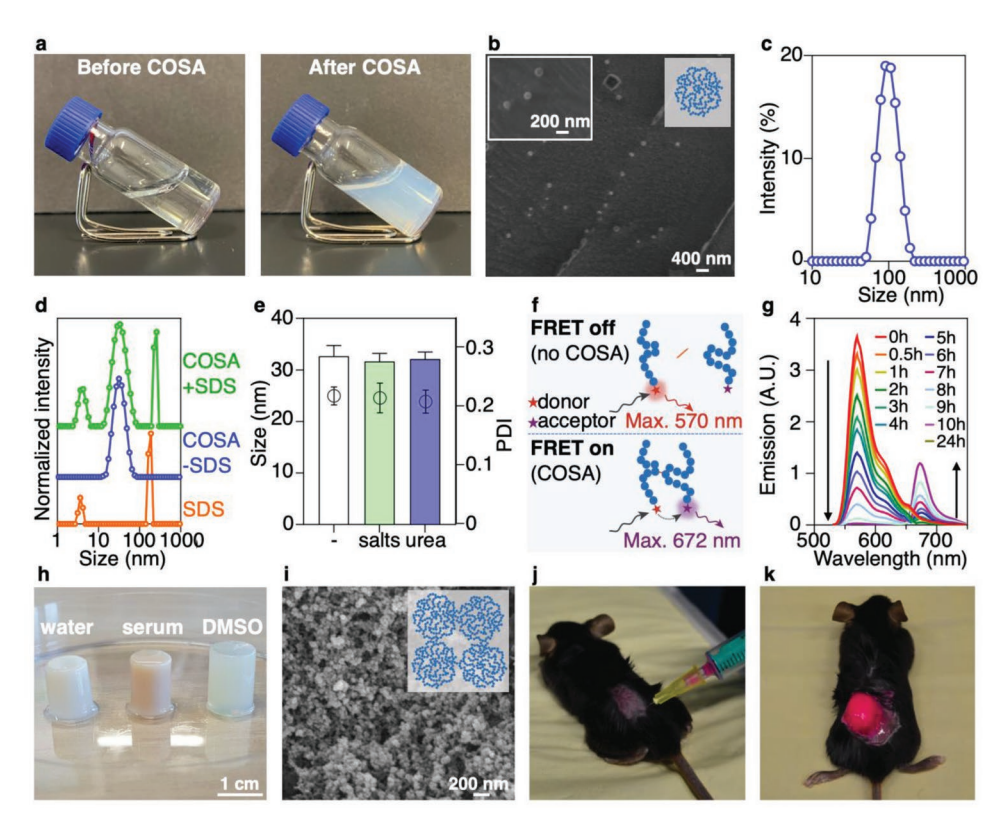


Figure 2. Nano- and microscale hydrogel formation from pOPMA via the COSA. a) Photographs of a water solution of pOPMA and ADH before and after the COSA. b,c) CryoSEM images and DLS size distribution plot of pOPMA nanogels. d) DLS size distribution plots of pOPMA nanogels prepared in the presence of SDS. Green, blue, and orange curves for COSA with SDS, COSA without SDS, and SDS alone. e) Size and polydispersity index (PDI) of pOPMA nanogels formed in the presence of salts (green) and urea (blue). f) Schematic depiction of FRET induced by the COSA of pOPMA chains labeled with Alexa-555 and Alexa-647. g) Emission spectra of pOPMA-bond Alexa-555 and Alexa-647 during COSA (excitation wavelength at 520 nm). h) Photograph of macroscopic pOPMA gels in water (pH 7.4), mouse serum, and DMSO. i) SEM image of a pOPMA hydrogel. j,k) Needle injection and in situ gelation of pOPMA and ADH (mixed with rhodamine B for visualization) in mice.

When increasing the DC, macroscopic gels are obtained in aqueous and organic solvents at 100% DC and 40 mg mL-1 polymer (Figure 2h). The macroscale gels are composed of pOPMA nanogels (Figure 2i). pOPMA has a remarkably broad range of gelation concentration, from 300 to 0.75 mg mL<sup>-1</sup> (100% DC, in phosphate-buffered saline (PBS) 6.5), and forms hydrogels with a great range of stiffness (Figure S15, Supporting Information). The gelation is characterized by infrared spectroscopy and the spectra show the reduction of the absorption band at 1724 cm<sup>-1</sup> for ketone groups,<sup>[13]</sup> which indicates that ketone groups are consumed during the process (Figure S16, Supporting Information). In aqueous media, the gelation time of pOPMA is pH-dependent since H<sup>+</sup> catalyzes the crosslinking reaction.<sup>[15]</sup> The gelation time is highly tunable in the biologically relevant pH range from 3.0 to 8.5 (Figure S17, Supporting Information). The hydrazone-based gelation of pOPMA in water is a reversible process which is controlled by pH as shown in Figure S18 in the Supporting Information. Furthermore, when incubating a mono-hydrazide mimic of ADH or a ketone mimic of OPMA with the hydrogels, these compounds react with the materials and the hydrogels are partially decrosslinked (Figure S19, Supporting Information). These data suggest that the hydrazone-based crosslinked networks are likely dynamic and exchange between ketone and hydrazone

possibly takes place. The hydrogel formation occurs in less than 5 min upon subcutaneous co-injection of pOPMA and ADH solutions in mice (Figure 2j,k).

# 2.3. Nanogel Size is Controlled by Crosslinking Reaction Rate

The size of pOPMA nanogels is easily controlled in the range of <10 to >100 nm by tuning the crosslinking reaction rate (Figure 3A). The crosslinking reaction rate and the size of yielded nanogels are modulated by regulating the pH (from 5.0 to 7.4; Figure 3B). The size modulation also works by adding an organic catalyst, aniline, to promote hydrazone formation (Figure S20, Supporting Information).[16] We obtain pOPMA nanogels (15 mg mL<sup>-1</sup> polymer) with sizes between 8 and 103 nm (20% DC), or 15 to 147 nm (30% DC), at the pH value ranging from 7.4 to 5.0. pOPMA nanogels of small and large size have similar levels of FRET between pOPMA-bound Alexa-555 and Alexa-647 (Figure S21, Supporting Information), indicating that the small nanogels are based on multiple polymer chains but not on intramolecularly crosslinked single polymer chains. The crosslinking rate-controlled size modulation is proposed to be due to the change of the ratio between intramolecular and intermolecular crosslinking. When polymer

15214095, 2022, 39, Downloaded

from https://onlinelibrary.wikey.com/doi/10.1002/adma.202109701 by Rwth Aachen Hochschulbibliothe, Wiley Online Library on [19/06/2023]. See the Terms

ons) on Wiley Online Library for rules of use; OA articles are governed by the applicable Creative Commons

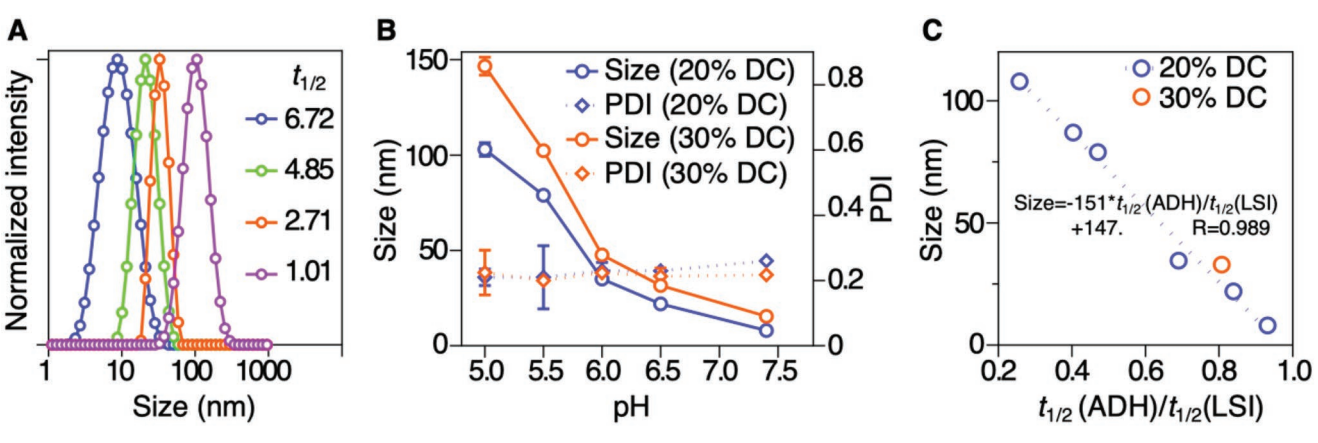


Figure 3. Size control of pOPMA nanogels formed via the COSA by changing the crosslinking rate. A) DLS size distribution plots of pOPMA nanogels synthesized at different crosslinking reaction rates. The reaction rate is characterized by the half-life (t<sub>1/2</sub>) of ADH consumption. B) Size and PDI of pOPMA nanogels formed at pH ranging from 5.0 to 7.4 (15 mg mL $^{-1}$  of polymer, 20% or 30% of DC). C) Linear correlation between the size and the ratio of  $t_{1/2}$  of ADH consumption and  $t_{1/2}$  of the LSI increase. R: linear correlation coefficient.

chains collide during the crosslinking reaction, the chance of intermolecular crosslinking is higher at faster reaction rates, which leads to the scenario that more chains are crosslinked together and therefore larger nanogels are formed. At slower reaction rates, the chance of intermolecular crosslinking is lower, which results in smaller nanogels. The size tuning of pOPMA nanoparticles is a well-controlled process with a linear correlation (Figure 3C, R = 0.989) between size and the ratio of  $t_{1/2}$  of ADH consumption (Figure S22, Supporting Information) and  $t_{1/2}$  of the light scattering intensity (LSI) increase during

COSA (Figure S23, Supporting Information). The size of nanogels with 30% DC also fits well in the correlation derived from nanogelation at 20% DC (Figure 3C).

#### 2.4. Covalent Microgel Self-Assembly for 3D Printing

The COSA enables covalent self-assembly of pOPMA microgels prepared using microfluidics via flow focusing droplet formation (Figure 4A and Figure S24, Supporting Information).

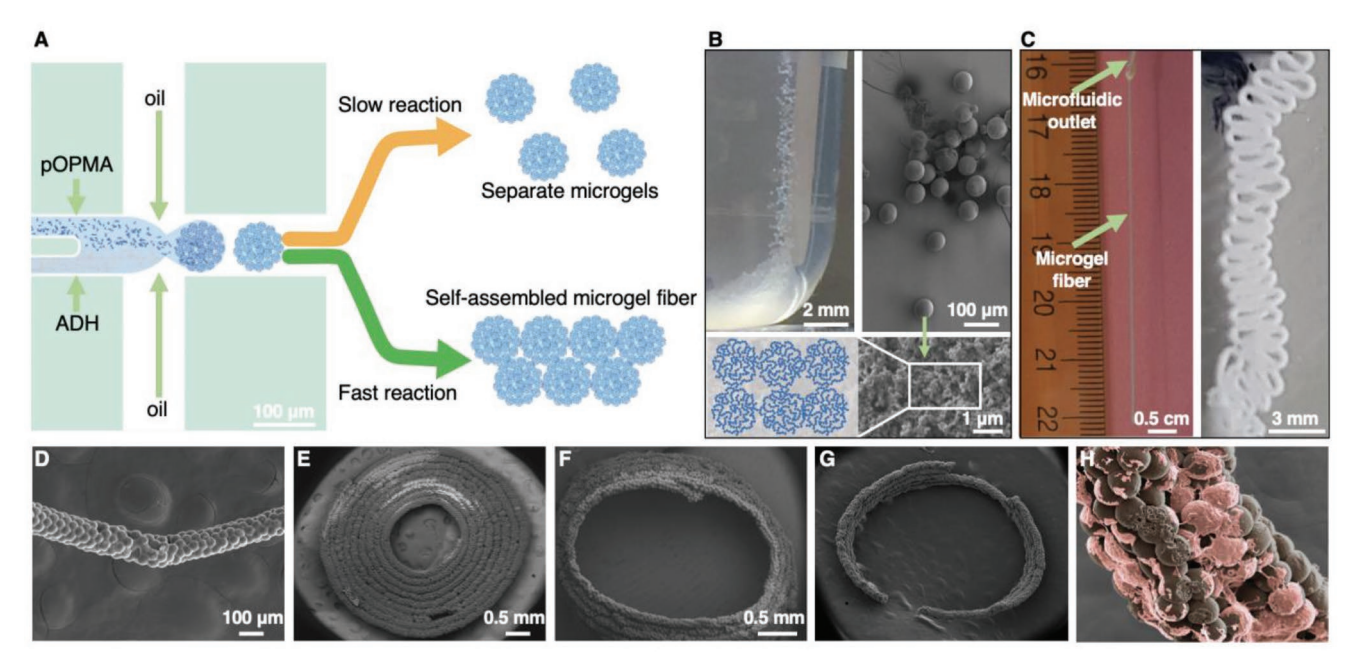


Figure 4. pOPMA microgels hierarchically assemble and are 3D printed as porous scaffolds. A) Schematic illustration of the microfluidic fabrication of pOPMA microgels of the dispersed phase at high and low pH values, resulting in separate microgels or microgel fibers. B) Separate microgels (left) produced via microfluidics and SEM images of the microgels (right) show that they are composed of nanogels (bottom). C) pOPMA microgels self-assemble into a fiber in the microfluidic outlet (left), which is printed on a glass plate (right), D-G) SEM images of pOPMA microgel-based fibers (D), which are printed as planar (E) and 3D porous scaffolds (F,G). H) SEM image of L929 fibroblast cells (color-coded in pink) spreading on the surface and in the pores of a pOPMA-microgel-based fiber after modification with 2-(aminooxy)ethanamine.



www.advancedsciencenews.com



www.advmat.de

materials are highly cytocompatible (Figures S27 and S28, Supporting Information).

pOPMA and ADH solutions are separately injected in two inlets, which are mixed and then cut by a continuous oil phase to form droplets (Figure 4A). At a high pH of the dispersed phase. i.e., slow ketone-hydrazide crosslinking rate, separate pOPMA microgels are produced (Figure 4B and Movies S1 and S2, Supporting Information). Interestingly, by lowering the pH of the dispersed phase and therefore accelerating the crosslinking reaction, pOPMA microgels covalently self-assemble inside the microfluidic outlet to form fibers (Figure 4A,C and Movie S3, Supporting Information). SEM analysis shows that the fibers are composed of interconnected microgels (Figure 4D). The formed fibers in the microfluidic outlet are printed into macroscopic planar and mechanically stable free-standing 3D porous scaffolds composed of multiple layers of fibers (Figure 4E-G). The pOPMA porous scaffolds are highly potential materials for tissue engineering. Although pOPMA does not interact with cells, it can be easily modified with functional groups to promote cell attachment and growth. We incubate pOPMA porous scaffolds within a 2-(aminooxy)ethanamine solution. The aminooxy group of 2-(aminooxy)ethanamine efficient reacts with pOPMA (native or crosslinked) to introduce cationic -NH<sub>3</sub><sup>+</sup> groups to the scaffolds (Figures S25–S27, Supporting Information). Afterward, fibroblast cells incubated with the scaffolds adhere to and spread on the surface and in the pores of the scaffolds (Figure 4H).

We here show a controlled self-assembly of a simple ketone homopolymer driven by covalent crosslinking, which is employed as a new strategy to fabricate nano- to macroscale hydrogels. We demonstrate the robust and highly controlled formation of the homopolymer-based nanogels, which further assemble into macroscale hydrogels with higher degrees of crosslinking. The crosslinking rate controls the size of the nanogels and microscale self-assembly behavior of granular gels.

The controlled covalent self-assembly is realized with a unique ketone homopolymer, pOPMA. It is based on the simplest methacrylamide monomer containing a ketone group and is structurally similar to one of the most widely used biomedical polymers, poly(*N*-(2-hydroxypropyl) methacrylamide), [17] whose hydroxyl group is replaced by ketone. Although there is only one group difference between the two polymers, the ketone group in pOPMA introduces several key properties for the novel covalent self-assembly approach and related applications. These properties include its selective and potent reactivity, biocompatibility, and hydrophilicity. Ketone is polar and facilitates water solubilization of the polymer. pOPMA is, to the best of our knowledge, the only ketone homopolymer with high water solubility (>300 mg mL<sup>-1</sup> in PBS 7.4). Ketone is highly biocompatible and chemically more stable than another carbonyl group, aldehyde. The latter causes high toxicities including protein denaturation and DNA damage.[18] Ketone is highly reactive toward amines with increased nucleophilicity (i.e., the α-effect), including hydrazide, hydrazine, and aminooxy. These groups undergo click reactions with ketone in an efficient and clean manner, which proceeds in aqueous solvents and is catalyzed by H<sup>+</sup>,<sup>[15]</sup> with water as the side product. These reactions are considered bioorthogonal and can be applied in living systems.[19] As shown in our study, pOPMA and pOPMA-based

Nanogels are an important class of delivery systems for small molecule and macromolecular drugs.[20,21] The covalent self-assembly of pOPMA enables a novel strategy of nanogel formulation. Current fabrication strategies of nanogels mostly employ physical means such as micromolding, inverse miniemulsion, microfluidics, and inverse nanoprecipitation strategies.[22-24] These methods involve organic solvents and/or surfactants which may cause denaturation of fragile payloads such as proteins<sup>[25]</sup> and have to be removed after formulation. Moreover, nanogelation can be induced by physical interactions between amphiphilic polymer chains, followed by chemical crosslinking. For example, amphiphilic copolymers composed of hydrophilic polyethylene glycol methacrylate repeating units and hydroponic repeating units of pyridyldisulfide, [26] pentafluorophenyl acrylate,<sup>[27]</sup> or *p*-nitrophenylcarbonate<sup>[28]</sup> self-assembled in aqueous solutions into nanogels and were chemically crosslinked via the reactive repeating units. The nanogelation is solvent-dependent, which is disadvantageous for loading macromolecular drugs when organic solvents are needed.[29] Compared to other physico-chemical gelation methods leading to macroscale gels without control of size, [30,31] COSA is highly controllable and provides a practical strategy to directly synthesize nano-to-macroscale gel materials, even ultra-small polymeric nanogels that are generally challenging to synthesize.[32] Our system is featured by its covalently induced self-assembly, single homopolymer composition, nonsolventdependence, multiscale gel formation, crosslinking rate-controlled size, and self-assembly behavior, which are substantially different from previous reports and are highly favorable for biomedical applications.

The covalent self-assembly of pOPMA also provides a facile and direct method for 3D printing of porous scaffolds composed of granular hydrogels. Biomaterial scaffolds hold crucial importance in tissue engineering. Recently, porous scaffolds based on microgels have shown great advantages than conventional scaffolds, which can highly promote cell migration in the scaffolds and nutrition exchange via the large porosity.<sup>[33–37]</sup> The state-of-the-art fabrication methods for such porous scaffolds begin with the production of microgels which are injected to the site of action[33] or 3D printed,[38-40] and additional crosslinking chemistry is applied to stabilize the scaffolds. Such two-step process not only adds to the fabrication complexity of microgel scaffolds, but also some crosslinking chemistry (e.g., UV-induced) may be harmful to living cells or inapplicable in vivo. These issues are well addressed with the covalent polymer self-assembly. In our approach, microgel-based fibers are directly fabricated from microfluidics and are flexibly printed into various 3D structures. And such advanced materials engineering is simply enabled by lowering the fabrication pH to trigger microgel assembly in the outlet of the microfluidic system. The covalently self-assembled microgels result in highly stable scaffolds with chemical crosslinks between the particles. In addition, the scaffolds can be easily modified with different functional molecules to create interactions with cells, which is crucial for tissue engineering and which is not easily achievable with other polymers.

www.advancedsciencenews.com



www.advmat.de

#### 3. Conclusion

We have established a novel and straightforward covalent polymer self-assembly strategy for biomaterials engineering. Our strategy is mechanistically different from conventional non-covalent self-assembly that is associated with several drawbacks such as low stability, difficulty in the control of the process, and complexity in fabrication techniques. We show in this work that the covalent self-assembly can address these challenges with its simple and environmentally friendly fabrication conditions and better control of the physico-chemical properties of the materials, e.g., size and morphology. The novel covalent polymer self-assembly will have broad applications in materials synthesis for biomedical engineering including drug delivery and tissue engineering.

## **Supporting Information**

Supporting Information is available from the Wiley Online Library or from the author.

# Acknowledgements

The authors acknowledge funding support by German Research Foundation (DFG: SH1223/1-1; LA 2937/4-1; GRK/RTG 2375: Tumortargeted Drug Delivery (331065168); SFB1066; SFB985: project B5), by China Scholarship Council (CSC: 201508150063), by the European Research Council (ERC: Meta-Targeting (864121); BeaT-IT (101040996)), by the Excellence Strategy of the Federal Government and the Länder ((DE-82)EXS-SF-OPSF580). No specific ethical approval was required for the experiments demonstrated in Figure 4, as a control post-mortem mouse that had been used in another study was reused in this work.

Open access funding enabled and organized by Projekt DEAL.

## **Conflict of Interest**

The authors declare no conflict of interest.

#### **Author Contributions**

Y.S. conceived and supervised the project. Y.S. and X.B. designed the experiments, solved technical issues, and analyzed the experimental results. X.B. performed the experiments. Q.S., H.C., and L.P.B.G. contributed to the experiments. T.L., L.D.L, F.K., and S.W. provided feedback on the project and manuscript writing.

## **Data Availability Statement**

The data that support the findings of this study are available from the corresponding author upon reasonable request.

## **Keywords**

3D printing, covalent self-assembly, ketone homopolymers, microgels, nanogels

Received: November 29, 2021 Revised: July 4, 2022 Published online: August 23, 2022

- [1] G. M. Whitesides, B. Grzybowski, Science 2002, 295, 2418.
- [2] M. Muthukumar, C. K. Ober, E. L. Thomas, Science 1997, 277, 1225.
- [3] T. Aida, E. W. Meijer, S. I. Stupp, Science 2012, 335, 813.
- [4] K. Tao, P. Makam, R. Aizen, E. Gazit, Science 2017, 358, eaam9756.
- [5] F. G. Omenetto, D. L. Kaplan, Science 2010, 329, 528.
- [6] Z. L. Wu, T. Kurokawa, S. Liang, H. Furukawa, J. P. Gong, J. Am. Chem. Soc. 2010, 132, 10064.
- [7] A. F. Mason, B. C. Buddingh, D. S. Williams, J. C. M. van Hest, J. Am. Chem. Soc. 2017, 139, 17309.
- [8] R. Freeman, M. Han, Z. Alvarez, J. A. Lewis, J. R. Wester, N. Stephanopoulos, M. T. McClendon, C. Lynsky, J. M. Godbe, H. Sangji, E. Luijten, S. I. Stupp, *Science* 2018, 362, 808.
- [9] J. Cai, C. Li, N. Kong, Y. Lu, G. Lin, X. Wang, Y. Yao, I. Manners, H. Oiu, *Science* 2019, 366, 1095.
- [10] H. S. Sasmal, A. Halder, H. S. Kunjattu, K. Dey, A. Nadol, T. G. Ajithkumar, P. Ravindra Bedadur, R. Banerjee, J. Am. Chem. Soc. 2019, 141, 20371.
- [11] K. I. Min, G. Yun, Y. Jang, K. R. Kim, Y. H. Ko, H. S. Jang, Y. S. Lee, K. Kim, D. P. Kim, Angew. Chem., Int. Ed. 2016, 55, 6925.
- [12] H. V. Schroder, Y. Zhang, A. J. Link, Nat. Chem. 2021, 13, 850.
- [13] Y. Shi, C. F. van Nostrum, W. E. Hennink, ACS Biomater. Sci. Eng. 2015. 1, 393.
- [14] H. S. Sasmal, S. Bag, B. Chandra, P. Majumder, H. Kuiry, S. Karak, S. Sen Gupta, R. Banerjee, J. Am. Chem. Soc. 2021, 143, 8426.
- [15] D. K. Kolmel, E. T. Kool, Chem. Rev. 2017, 117, 10358.
- [16] A. Dirksen, S. Dirksen, T. M. Hackeng, P. E. Dawson, J. Am. Chem. Soc. 2006, 128, 15602.
- [17] J. Kopecek, P. Kopeckova, Adv. Drug Delivery Rev. 2010, 62, 122.
- [18] J. I. Garaycoechea, G. P. Crossan, F. Langevin, L. Mulderrig, S. Louzada, F. Yang, G. Guilbaud, N. Park, S. Roerink, S. Nik-Zainal, M. R. Stratton, K. J. Patel, *Nature* 2018, 553, 171.
- [19] E. M. Sletten, C. R. Bertozzi, Angew. Chem., Int. Ed. 2009, 48, 6974.
- [20] A. V. Kabanov, S. V. Vinogradov, Angew. Chem., Int. Ed. 2009, 48, 5418.
- [21] J. R. Clegg, A. S. Irani, E. W. Ander, C. M. Ludolph, A. K. Venkataraman, J. X. Zhong, N. A. Peppas, Sci. Adv. 2019, 5, eaax7946.
- [22] X. Zhang, S. Malhotra, M. Molina, R. Haag, Chem. Soc. Rev. 2015, 44, 1948.
- [23] J. K. Oh, R. Drumright, D. J. Siegwart, K. Matyjaszewski, Prog. Polym. Sci. 2008, 33, 448.
- [24] N. Hauck, T. A. Neuendorf, M. J. Mannel, L. Vogel, P. Liu, E. Stundel, Y. Zhang, J. Thiele, Soft Matter 2021, 17, 10312.
- [25] K. Fu, R. Harrell, K. Zinski, C. Um, A. Jaklenec, J. Frazier, N. Lotan, P. Burke, A. M. Klibanov, R. Langer, J. Pharm. Sci. 2003, 92, 1582.
- [26] J. H. Ryu, R. T. Chacko, S. Jiwpanich, S. Bickerton, R. P. Babu, S. Thayumanavan, J. Am. Chem. Soc. 2010, 132, 17227.
- [27] J. Zhuang, S. Jiwpanich, V. D. Deepak, S. Thayumanavan, ACS Macro Lett. 2011, 1, 175.
- [28] K. Dutta, D. Hu, B. Zhao, A. E. Ribbe, J. Zhuang, S. Thayumanavan, J. Am. Chem. Soc. 2017, 139, 5676.
- [29] A. W. Jackson, C. Stakes, D. A. Fulton, Polym. Chem. 2011, 2, 2500.
- [30] T. Yuan, J. Fei, Y. Xu, X. Yang, J. Li, Macromol. Rapid Commun. 2017, 38, 1700408.
- [31] K. Sano, R. Kawamura, T. Tominaga, N. Oda, K. Ijiro, Y. Osada, Biomacromolecules 2011, 12, 4173.
- [32] D. Mecerreyes, V. Lee, C. J. Hawker, J. L. Hedrick, A. Wursch, W. Volksen, T. Magbitang, E. Huang, R. D. Miller, Adv. Mater. 2001, 13, 204.
- [33] D. R. Griffin, W. M. Weaver, P. O. Scumpia, D. Di Carlo, T. Segura, Nat. Mater. 2015, 14, 737.
- [34] A. Sinclair, M. B. O'Kelly, T. Bai, H. C. Hung, P. Jain, S. Jiang, Adv. Mater. 2018, 30, 1803087.
- [35] C. W. Visser, T. Kamperman, L. P. Karbaat, D. Lohse, M. Karperien, Sci. Adv. 2018, 4, eaao1175.

15214095, 2022, 39, Downloaded from https://onlinelibrary.wiley.com/doi/10.1002/adma.202109701 by Rwth Aachen Hochschulbibliothe, Wiley Online Library on [19/06/2023]. See the Terms

www.advancedsciencenews.com



www.advmat.de

- [36] A. S. Mao, B. Ozkale, N. J. Shah, K. H. Vining, T. Descombes, L. Zhang, C. M. Tringides, S. W. Wong, J. W. Shin, D. T. Scadden, D. A. Weitz, D. J. Mooney, Proc. Natl. Acad. Sci. USA 2019, 116,
- [37] A. S. Caldwell, B. A. Aguado, K. S. Anseth, Adv. Funct. Mater. 2020, *30*, 1907670.
- [38] M. Shin, K. H. Song, J. C. Burrell, D. K. Cullen, J. A. Burdick, Adv. Sci. 2019, 6, 1901229.
- [39] C. B. Highley, K. H. Song, A. C. Daly, J. A. Burdick, Adv. Sci. 2019, 6, 1801076.
- [40] Q. Li, Y. W. Zhang, C. F. Wang, D. A. Weitz, S. Chen, Adv. Mater. **2018**, *30*, 1803475.

Adv. Mater. 2022, 34, 2109701